arXiv:cond-mat/0105511v1 [cond-mat.mes-hall] 26 May 2001

Discrete saturation thickness and anomalous potential height of native ultrathin aluminum oxide tunnel barriers

K. Gloos, P. J. Koppinen, and J. P. Pekola
Department of Physics, University of Jyväskylä, PO Box 35 (YFL), FIN-40351 Jyväskylä, Finland
(February 1, 2008)

We have investigated planar metal - insulator - metal tunnel junctions with aluminum oxide as dielectricum. These oxide barriers were grown on an aluminum electrode in pure oxygen at room temperature till saturation. We observed discrete barrier widths separated by $\Delta s \approx 0.38\,\mathrm{nm}$, corresponding to the addition of one layer of oxygen atoms. The minimum thickness of $s_0 \approx 0.54\,\mathrm{nm}$ is due to a double layer of oxygen. We found a strong and systematic dependence of the barrier height Φ_0 on the thickness s like $\Phi_0 \approx 2.5\,\mathrm{eV}/s^2(\mathrm{nm})$, which nearly coincides with the kinetic electron energy $E = h^2/2ms^2$ for which the deBroglie wavelength matches the width of the barrier.

73.40.Gk, 73.40.Rw, 73.61.Ng

Aluminum oxide (AlO_x) is one of the standard construction materials for tunneling barriers because it is easily and reliably being formed. It is important for applications like single-electron transistors [1] and Coulomb-blockade thermometers [2]. Aluminum oxide is also a promising candidate to replace SiO_2 based gate dielectrics in miniaturized electronic circuits, see for example Ref. [3]. Although many experiments take advantage of AlO_x tunnel barriers, few reports focus on their intrinsic properties. The conventional point of view on these properties summarizes as follows: *i*) Almost any conductance per area can be achieved by simply choosing the right oxidation pressure and time. *ii*) The typical height of the tunnel barrier is about 2 eV. But experimental data vary from below 0.1 eV up to 8.6 eV [4–6]. *iii*) The dielectric constant ϵ of the aluminum oxide barrier is smaller than that of bulk Al_2O_3, which is around 4.5 - 8.9 at around 295 K [7]. Like the height, ϵ does not seem to be a well-defined property of AlO_x.

In view of the importance of these tunnel barriers we have investigated them in more detail. We show that the height of ultrathin aluminum oxide barriers is *not at all* related to the band gap of bulk Al_2O_3. Instead, it seems to be a purely geometrical effect set by the lowest kinetic electron energy for which the deBroglie wavelength is smaller than the width s of the barrier. This interpretation is supported by resolving, for the first time, the layer-by-layer thickness of the saturated oxide barrier.

The most simple picture of a tunnel junction assumes an s wide rectangular barrier of height Φ_0 across which electrons tunnel. In Wentzel-Kramers-Brillouin (WKB) approximation the conductance per area at zero bias and at low temperatures becomes [8]

$$g_0 = \frac{e^2\sqrt{2m\Phi_0}}{h^2 s}\,\exp\left(\frac{2s}{\hbar}\,\sqrt{2m\Phi_0}\right). \qquad (1)$$

The first order correction increases the conductance quadratically with bias voltage V like [8]

$$g(V) = g_0\,(1 + V^2/V_0^2) \qquad (2)$$

with $V_0^2 = (4\hbar^2/e^2m)\Phi_0/s^2$. Equations 1 and 2 can be used to estimate s and Φ_0 of the junction. In general, image forces act on the electrons as they move through the barrier from one metal electrode to the other. They distort the potential distribution of real junctions, as described by the standard Simmons model [8]. The barrier height and its width determine then, together with the dielectric constant ϵ, the zero-bias conductance g_0 and the slope parameter V_0. Zero-bias anomalies (ZBA) omitted so far are discussed below.

We fabricated 99 samples on an oxidized Si substrate, using the standard two-angle shadow evaporation technique to deposit the metal electrodes in an ultra-high vacuum (UHV) chamber at a rate of 0.3 nm/s. The samples had $N = 12$ nominally identical junctions in series, each of $A = 2 \times 2\,\mu\mathrm{m}^2$ cross-section. Electrodes were evaporated through a 300 nm thick Si_3N_4 mask as shown in the inset of Fig. 2. A 25 μm diameter Al wire separated the mask from the substrate. By using a metal wire as a spacer we avoid organic material near the sample which could otherwise contaminate the oxide layer or the electrodes. The first Al layer, either pure Al or its alloys with Cu, Au, or Nb, was exposed to pure oxygen at ambient temperature ($\sim 295\,\mathrm{K}$) to form a thin insulating AlO_x barrier. About $5 \cdot 10^4$ Pa oxygen pressure was applied for 30 minutes in the loading chamber of the UHV system. Then the second electrode (Al, Cu, Nb, Au, or a mixture between two of those metals) was evaporated. The thickness of the electrodes was about 90 nm. We have found no systematic dependence of the final tunnel conductance per area on oxygen pressure, oxidation time, evaporation rate, junction area, or thickness of the metal electrodes when the relevant parameters were varied by a factor of two. In this respect the experiments are quite reproducible and represent the saturation thickness of the barrier at 295 K in pure oxygen.

Both the size of the area and the number of junctions are a compromise: The area is large enough to be reliably measured, but sufficiently small to show a resolvable Coulomb blockade signal at 4.2 K when the sample is in

the liquid helium of a transport dewar. We have chosen this condition to make a reliable comparison and to minimize the turn-around time. The number of junctions N still allows sufficiently large voltages to be applied across each junction using conventional electronic equipment. But simultaneously it reduces the risk of external high voltage spikes destroying the junctions.

From the sheet resistance of the shorted junctions - obtained either by omitting the oxidation process or when the tunnel barriers have been short-circuited by a large bias voltage - we estimate a residual electrical resistivity of the evaporated metals of $4 - 10\,\mu\Omega$cm at 4.2 K and a resistance ratio between 295 K and 4.2 K of around 1.5, indicating a good quality of the electrodes, both for the pure metals and the alloys.

The differential conductance dI/dV was recorded by applying a small low-frequency (~ 100 Hz) ac voltage dV superposed on the bias voltage V to the junction and detecting the current modulation dI with the help of a lock-in amplifier. Results are always presented as the voltage drop per junction and the conductance per area A of the junctions $g = (1/A)dI/dV$.

Figure 1 shows typical $dI(V)/dV$ spectra of an Al-oxide-Cu and an Al-oxide-Au tunnel contact at $T = 4.2$ K. Both have the same characteristic zero-bias anomalies. The essential difference between them is the strength of the V^2-dependence at larger voltages. It is basically this difference which indicates the thinner (Au contact) and the thicker (Cu contact) barrier.

Since most of our junctions have normal electrodes (at $T = 4.2$ K), we rely on several observations to ensure quantum tunnelling: *i*) The typically $\sim 15\%$ reduction of the conductance on cooling from 295 K to 4.2 K [9], which has been proposed recently as a good tunnelling indicator [10]. *ii*) The V^2-dependence of the conductance. *iii*) Several zero-bias anomalies (ZBA) appear at lower voltages. They can be attributed to inelastic electron-phonon scattering in the barrier [6]. We believe that the well-pronounced characteristic 110 meV anomaly, which we have regularly observed at thin barriers with $s \leq 1.0$ nm, indicates the high quality of those tunnel junctions. *iv*) Several Al-oxide-Nb junctions, prepared at the same conditions as the other samples, showed the expected superconducting anomalies. *v*) The known shape of the Coulomb blockade spectrum, see below.

Partial Coulomb blockade at $T = 4.2$ K can be resolved as long as the background zero-bias anomaly has a conductance maximum at $V = 0$. Figure 1 c) shows that the spectra normalized to the smoothed background fit well the expected shape due to Coulomb blockade. This also indicates that the $N = 12$ junctions are rather identical. In both cases the width of the anomaly [2] $V_{1/2} = 5.44\,k_{\rm B}T/e$ derived from the fit curve corresponds to a nominal temperature of 4.4(3) K, in good agreement with the experimental 4.2 K. Because of the large contact area the Coulomb blockade anomaly is quite small. Nevertheless, its relative size can be used to derive the capacitance of the junctions C [2]. From that we estimate an average dielectric constant of $\epsilon \approx 4$ for the parallel-plate geometry with $C = \epsilon\epsilon_0 A/s$.

Surprisingly, most of the tunnel spectra are quite symmetric like that in Fig. 1, even when the electrodes are of different metals, implying that the tunnel barriers are likewise symmetric. Therefore we did not apply the generalized Simmons model for junctions with an asymmetric barrier [11], but always symmetrized the spectra to obtain the average barrier heights. Plotting the differential conductance versus V^2 reveals a linear relationship above the 110 meV anomaly from which V_0 can be extracted (the Al-oxide-Au samples had a very small V^2 contribution, making the analysis more difficult). Fitting the spectra above the ZBA using Simmons model and the average $\epsilon = 4$ allows us to determine s and Φ_0. The final result depends only weakly on the absolute value of ϵ if this is varied by $\pm 50\%$, and the complete analysis indicates a temperature dependence of ϵ and/or Φ_0 [12].

Figure 2 summarizes our main findings. First, the barrier height depends very strongly and systematically on the thickness s of the barrier like $\Phi_0 \propto 1/s^2$. These data clearly demonstrate that Φ_0 is neither related with the band gap of bulk Al_2O_3 nor to the work function of the different metals. Second, data points accumulate at certain values of the thickness, following a regular pattern with a $\Delta s \approx 0.38(5)$ nm spacing as shown in the histogram in Fig. 3. Such a spacing could be expected for a homogeneously grown oxide layer, built up basically by adding one layer of oxygen atoms to an already existing one (the Al atoms are much smaller than the O atoms). The smallest observed thickness $s_0 \approx 0.54(5)$ nm corresponds then to two oxygen layers as proposed theoretically in Ref. [13]. This minimum thickness is also consistent with recent observations of stable 0.6 nm thick Al_2O_3 films grown on a Si substrate [3] and 0.59 nm Al_2O_3 films on Ta [14]. The discreteness of the width s with reasonable absolute values strongly supports our way to derive the width, and therefore also the barrier height.

We note here that only Al-oxide-Au junctions were of s_0 type, all other samples with pure Al base electrodes, like Al-oxide-Al and Al-oxide-Cu, were mainly of s_1 type, as shown in Fig. 3. Samples with Al alloys as base electrode, like $Cu_{0.5}Al_{0.5}$, were mostly of s_2 type, but a considerable fraction of them was of s_1 and s_3 type. The barrier of samples with a pure Al base electrode seems to be quite homogenous, while those of Al alloy samples could be inhomogeneous, resulting in an average thickness between s_1 and s_2, as seen in the histogram. Obviously, thicker barriers are more easily being formed on Al alloys with their degraded (irregular) surface structure than on pure Al. On the other hand, the preference of the Au samples to form very thin barriers could result from the fact that Au is difficult to oxidize unlike Al or Cu. After oxidation, the top-most layer is probably

chemisorbed oxygen. When evaporating Al or Cu as the second electrode, these oxygen atoms form bonds with the metals, but desorb easily when Au is evaporated.

Especially the thin oxide layers with s_0 and s_1 have a well-pronounced 110 meV zero-bias anomaly as shown in Fig. 1. This anomaly characterizes the surface (or longitudinal) phonons of crystalline Al_2O_3 (sapphire), see for example Ref. [15]. Thus in these samples the oxygen ions are fully bound in a regular crystal lattice and not only chemisorbed. Chemisorption may be the case for the thicker barriers. For them the 110 meV anomaly is strongly suppressed and an anomaly at around 50 meV appears. A second reason for this suppression could be inhomogeneities in the barrier. This is consistent with observing noisier spectra at those junctions, indicating more defects.

Several other experiments either contradict or support our findings. The supporting ones use a sample structure similar to ours, namely metal-oxide-metal tunnel junctions: Lau and Coleman [6] investigated thermally and plasma-discharge grown aluminum oxide barriers while Barner and Ruggiero [5] sputter-deposited Al_2O_3 tunnel barriers. In both cases the absolute values as well as the thickness dependence of the barrier height $\Phi_0(s)$ agree well with our data. Especially the latter report extends our data set to significantly larger s. The contradicting experiments use different sample setups, metal-oxide-semiconductors juctions: Ballistic electron emission spectroscopy on AlO_x found 3.90(3) eV high barriers for 8 nm oxide thickness [16], compared to our (extrapolated) 40 meV. Internal photoemission gave $\Phi_0 = 3.25(8)$ eV for $5-15$ nm wide barriers [17]. According to Ref. [16] there is almost no difference of the barrier height when AlO_x is replaced by SiO_2. But according to Ref. [17] the numbers are different, namely 4.25(5) eV and 3.25(8) eV for SiO_2 and AlO_x, respectively.

The different results for the different kind of setups could indicate that boundary conditions matter. And this could lead to a tentative explanation for the well-defined 'cut-off energy' $\Phi_0(s)$ of our samples. The experimental $\Phi_0(s)$ in Fig. 2 marks roughly the kinetic energy

$$E = \frac{h^2}{2ms^2} \approx \frac{1.5\,\mathrm{eV}}{s^2(\mathrm{nm})} \qquad (3)$$

at which the deBroglie wavelength of the electrons becomes smaller than the width s of the barriers. The cut-off would then be simply induced by an electronic resonance phenomenon inside the barrier.

We have tried to verify independently the potential height by measuring the current-voltage characteristics to higher voltages. Figure 4 shows the voltage V_b at which the tunnel current raises dramatically, exceeding ~ 1 mA. The junctions are then usually destroyed, resulting in either a short or an open circuit. However, this breakdown voltage V_b seems to be smaller than the one expected for field emission. Up to about $\Phi_0 = 4$ eV the breakdown voltages are closely correlated with the potential height, thus supporting the magnitude of Φ_0 derived from the spectra at low bias voltages. The larger Φ_0 above 4 eV requires additional considerations because of the obvious trend of V_b to saturate at around 2.5 V (the Al-oxide-Au samples had slightly, but systematically, larger V_b than the Al-oxide-Cu or Al-oxide-Al samples). Either these large barrier heights are wrong or we face a new effect. The latter is probably the case because of the huge electrical breakdown fields $E_b = V_b/s$, approaching ~ 5 GV/m at small s. Compared to that, typical literature data for AlO_x junctions have much lower $E_b \approx 0.1-1$ GV/m at most [18]. A breakdown field which decreases with increasing gap between the electrodes is a well-known, yet not fully understood, phenomenon in vacuum high-voltage insulation [19]. The 2.5 V upper bound of V_b could be readily explained by the damage done due to the mechanical stress excerted by the electrical field. One could also speculate whether the extremely high tunnel current density $\sim 10^8$ A/m^2 just below V_b induces a high enough electron density inside the barrier that could transform the insulating AlO_x into a conducting metallic state. Whatever the right explanation, the large E_b confirms the excellent quality of our tunnel barriers with a very small number of defects that could act as weak spots.

Finally, the systematic $\Phi_0(s)$ dependence leads to a preferred transparency of the tunnel junctions for each saturation thickness which covers roughly two decades in conductance per area. A wider range of transparencies is difficult to achieve by just varying the thickness of the barriers.

We thank N. Kim for discussions. This work has been supported by the Academy of Finland under the Finnish Centre of Excellence Programme 2000-2005 (Project No. 44875, Nuclear and Condensed Matter Programme at JYFL) and by the European Commission under the Measurement and Testing activity of the Competitive and Sustainable Growth Programme (Contract G6RD-CT-1999-00119).

[1] H. Grabert and M. H. Devoret (eds.), *Single Charge Tunneling* (Plenum Press, New York, 1992).

[2] J. P. Pekola, K. P. Hirvi, J. P. Kauppinen, and M. A. Paalanen, Phys. Rev. Lett. **73**, 2903 (1994).

[3] M. Kundu, N. Miyata, and M. Ichikawa, Appl. Phys. Lett. **78**, 1517 (2001).

[4] K. H. Gundlach and J. Hölzl, Surface Science **27**, 125 (1971).

[5] J. B. Barner and S. T. Ruggiero, Phys. Rev. **B 39**, 2060 (1989).

[6] J. C. Lau and R. V. Coleman, Phys. Rev. **B 24**, 2985 (1981).
[7] R. E. Bolz and G. L. Tuve (eds.), *CRC Handbook of Tables for Applied Engineering Science*, (CRC Press, Boca Raton, Florida, 1983).
[8] J. G. Simmons, J. Appl. Phys. **34**, 1793 (1963).
[9] K. Gloos, R. S. Poikolainen, and J. P. Pekola, Appl. Phys. Lett. **77**, 2915 (2000).
[10] B. J. Jönsson-Åkerman, R. Escudero, C. Leighton, S. Kim, I. K. Schuller, and D. A. Rabson, Appl. Phys. Lett. **77**, 1870 (2000).
[11] W. F. Brinkman, R. C. Dynes, and J. M. Rowell, J. Appl. Phys. **41**, 1915 (1970).
[12] K. Gloos *et al.*, to be publ.
[13] D. R. Jennison, C. Verdozzi, P. A. Schultz, and M. P. Sears, Phys. Rev. **B 59**, R15605 (1999).
[14] P. J. Chen and D. W. Goodman, Surf. Sci. **312**, L767 (1994).
[15] I. Popova, V. Zhukov, and J. T. Yates, Jr. J. Appl. Phys. **87**, 8143 (2000).
[16] R. Ludeke, M. T. Cuberes, and E. Cartier, Appl. Phys. Lett. **76**, 2886 (2000).
[17] V. V. Afanas'ev, M. Houssa, A. Stesmans, and M. M. Heyns, J. Appl. Phys. **78**, 3073 (2001).
[18] C. S. Bhatia, G. Guthmiller, and A. M. Spool, J. Vac. Sci. Technol. **A 7**, 1298 (1989).
[19] W. T. Diamond, J. Vac. Sci. Technol. **A 16**, 707 (1998).

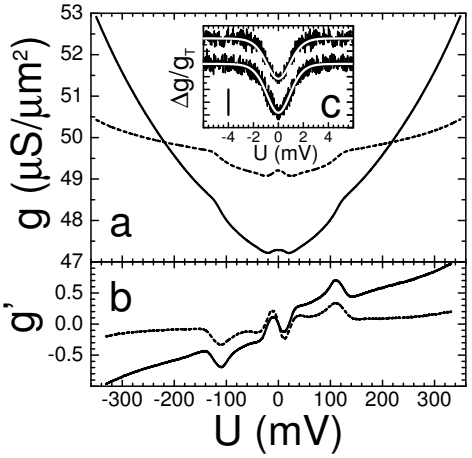

FIG. 1. a) Differential conductance $g = (1/A)dI/dV$ vs. voltage drop V for two typical tunnel junctions at $T = 4.2\,\mathrm{K}$. Solid line Al-oxide-Cu, dashed line Al-oxide-Au (not symmetrized original data). b) Second derivative $g' = dg/dU$ of the two spectra in arbitrary units. c) Coulomb-blockade anomaly of the two tunnel junctions. The change Δg of conductance due to Coulomb blockade has been normalized to the background conductance g_T. Solid white lines are theoretical predictions. The vertical bar indicates a 2×10^{-4} variation. From the size of the anomalies we estimate junction capacitances of about 0.22 pF and 0.18 pF and dielectric constants of $\epsilon \approx 5.6$ and 3.1 for the Cu (top) and the Au (bottom) sample, respectively.

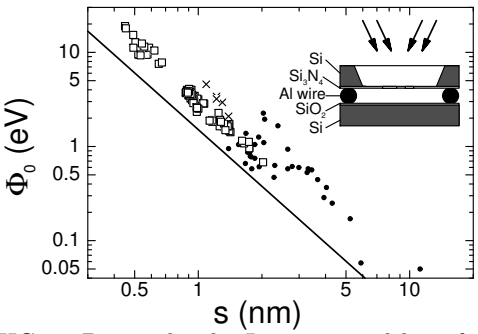

FIG. 2. Barrier height Φ_0 versus width s of aluminum oxide tunnelling barriers. The solid line represents Eq. 3. Solid circles are the data of Ref. [5] for sputter-deposited Al_2O_3 barriers. Crosses are averaged data from Ref. [6] for thermally or plasma-discharge oxidized Al. The inset shows our experimental setup to evaporate the metallic electrodes through a thin Si_3Ni_4 mask onto an oxidized Si substrate (not to scale). Arrows mark the two different evaporation angles before and after oxidation.

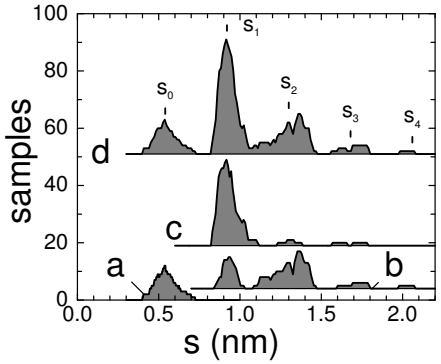

FIG. 3. Histogram of the number of samples falling inside a 0.1 nm wide interval around a barrier thickness s. A total of 99 samples have been measured. Trace a represents the Al-oxide-Au samples, trace b belongs to (M, Al)-oxide-M and (M, Al)-oxide-(Al, M) samples (M = Al, Cu, Au, or Nb), and trace c to the Al-oxide-M samples. Trace d is the sum of all samples. Traces b, c, and d are vertically displaced.

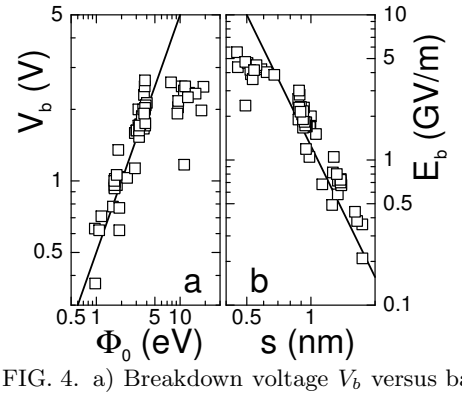

FIG. 4. a) Breakdown voltage V_b versus barrier height Φ_0 and b) breakdown field E_b versus barrier thickness s. The solid lines are $V_b = 0.5\,\Phi_0/e$ and $E_b = 1.25\,(\mathrm{GV/m})/s^3(\mathrm{nm})$, respectively.